Chapter 16
T4 Phage Replisome

Scott W. Nelson, Zhihao Zhuang, Michelle M. Spiering, and Stephen J. Benkovic

The bacteriophage T4 DNA replisome has been a useful model system for studying cellular DNA replication. Several decades of studies revealed that despite the variation in number and nature of individual proteins in the T4 replisome as compared to other model systems (*Escherichia coli* and yeast *Saccharomyces cerevisiae*), the fundamental components that constitute a functional replication fork in bacteriophage T4 faithfully represent other more complex replication systems (Fig. 16.1; Table 16.1). Therefore what has been learned from the T4 replisome can be extended to the replisomes of other organisms, including higher eukaryotes. One advantage of the T4 replisome as a model system is its manipulable complexity. The eight proteins that constitute the T4 replisome are the DNA polymerase (gp43), the clamp loader and clamp proteins (gp44/62 and gp45), the single-stranded DNA-binding protein (gp32), the primase and the helicase (gp61 and gp41), and the helicase-loading protein (gp59). These proteins form sub-complexes including DNA polymerase holoenzyme (gp43, gp45, and gp44/62), primosome (gp61, gp41, and gp59), and single-stranded DNA-binding protein (gp32). In this chapter we will discuss the properties of individual sub-complexes as well as the structural and functional aspects of their components. We will address how these complexes are assembled from individual proteins and how their functions are coordinated to ensure the efficient duplication of the T4 phage genome.

DNA Polymerase Holoenzyme

In bacteriophage T4 the DNA replisome is responsible for the rapid and accurate synthesis of genomic DNA. The core of the T4 replisome is the DNA polymerase (gp43, 898 a.a.), which catalyzes the incorporation of deoxynucleotides in the 5′ to 3′ direction. Like many other replicative DNA polymerases T4 gp43 also possesses a 3′ to 5′ exonuclease activity. The polymerase alone is not processive, i.e.,

S.J. Benkovic (✉)
Department of Chemistry, Pennsylvania State University, 414 Wartik Laboratory, University Park, PA 16802, USA
e-mail: sjb1@psu.edu

C.E. Cameron et al. (eds.), *Viral Genome Replication*,
DOI 10.1007/b135974_16,

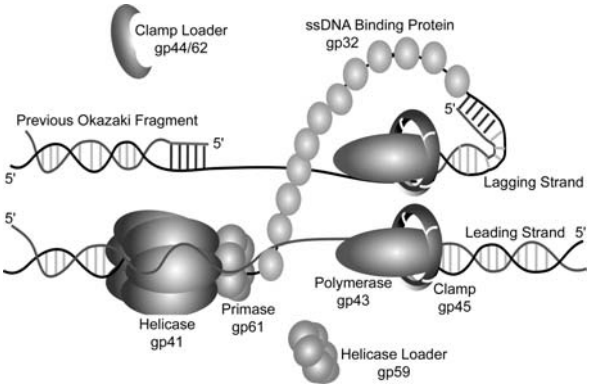

Fig. 16.1 Architecture of the bacteriophage T4 DNA replication complex. The T4 replication complex is composed of eight proteins that interact to synthesize DNA. In the current model, a helicase (gp41) and primase (gp61) form stacked hexameric rings that encircle the lagging DNA strand. This primosome complex is assembled with the aid of a helicase assembly protein, gp59. The helicase unwinds duplex DNA ahead of the polymerase while the primase synthesizes pentaribonucleotide primers for use by the lagging strand polymerase (gp43). Single-strand regions of DNA created from helicase activity are bound by gp32, a single-stranded DNA binding protein. Two trimeric gp45 proteins (which are loaded by the gp44/62 clamp loader complex) bind to the leading and lagging strand polymerases and increase their processivity.

Table 16.1 Replication and recombination proteins from T4 phage, *E. coli*, and *S. cerevisiae*

	T4 phage	*E. coli*	*S. cerevisiae*
Polymerase	gp43	α, ε, θ	Pol3, 31, 32, Pol2, Dpb(2–4)
Clamp	gp45	β	PCNA
Clamp loader	gp44, 62	γ, τ, δ, δ′, χ, Ψ	RFC(1–5)
Helicase	gp41	DnaB	Possibly Mcm(2–7)
Helicase loader	gp59	DnaC	Unknown
Primase	gp61	DnaG	pol1, 12, and Pri2, 1
ssDNA-binding protein	gp32	SSB	RPA, RPA70, 30, 14

it produces short DNA product strands during a single DNA-binding event (Mace and Alberts 1984). Efficient replication of the 168 kb T4 genome necessitates the formation of the DNA holoenzyme complex that has greatly increased stability on DNA. The formation of polymerase holoenzyme requires accessory proteins gp45 (228 a.a.) and gp44/62 (319/187 a.a.). gp45 is a toroid-shaped processivity factor with an inner diameter large enough to encircle duplex DNA. Once loaded onto duplex DNA the clamp acts as a platform that tethers gp43 to DNA through a topological linkage between the C-terminus of gp43 and one specific face of the gp45 toroid (Latham et al. 1997a,b; Goodrich et al. 1997). The loading of gp45 onto duplex DNA requires the clamp loader gp44/62. In T4 the clamp loader is a

complex of four gp44 and one gp62 subunits (Janzen et al. 1999). Besides the role of clamp loading gp44/62 also functions as a molecular chaperon for recruiting gp43 to assemble the functional holoenzyme (Trakselis et al. 2003a).

gp43 DNA Polymerase

To date the high-resolution structure of the T4 gp43 has not been reported. Nonetheless the X-ray crystal structure of the RB69 polymerase gp43 that shares 61% sequence identity to the T4 gp43 was solved by Steitz and coworkers. Such a high degree of amino acid sequence identity strongly argues for the conservation of three-dimensional structures between the two polymerases. Indeed a T4 gp43 structural model was generated with high confidence through a threading program (Xi et al. 2005a) and we will use the RB69 gp43 structure for an account of the structure and function of the T4 gp43.

Three RB69 gp43 structures were reported, including an apo form (Wang et al. 1997), a binary complex of gp43 and a primer–template DNA (Shamoo and Steitz 1999), and a ternary complex of gp43 with primer–template DNA and dTTP bound (Franklin et al. 2001). The gp43 polymerase belongs to the Pol α family. The structure of gp43 can be divided into five domains within a polypeptide chain of 903 residues. The N-terminal half of gp43 (residues 1–380) can be separated from the C-terminal half (residues 381–903) by truncation of the full-length protein (Lin et al. 1994). The N-terminal half of gp43 consists of an N-terminal domain and an exonuclease domain. The C-terminal half of gp43 adopts the common right-handed shape observed for DNA polymerases with three domains named finger, palm, and thumb. Overall the five domains form a disk with a noticeable hole in the center. The palm domain is the most conserved domain compared to other polymerases from the Pol I, Pol α, and reverse transcriptase families. The palm domain of gp43 is formed by a β-sheet that is flanked by two α-helices on one side. The three conserved aspartate residues (D411, D621, and D623) that are important for polymerase activity are located on three β-strands of the palm domain. Two of the conserved residues (D411 and D623) contribute to the binding of two metal ions. The phosphoryl transfer reaction catalyzed by gp43 is most likely through an associative transition state following the formation of a closed ternary complex of polymerase, DNA, and incoming dNTP. The ternary X-ray structure suggests that residue K560 in the finger domain together with the two metal ions bound by the conserved acidic residues in the palm domain help to stabilize the pentacovalent geometry and neutralize the additional negative charge on the equatorial oxygens developing in the transition state.

The finger domain of gp43 is formed by two long antiparallel helices (residues 471–572). In the apo-gp43 structure the finger domain adopts an open conformation protruding away from the backside of the disk formed by palm, thumb, and exonuclease domains. In the ternary complex of gp43 bound with primer–template DNA and dTTP, a drastic conformational change of the finger domain is evident where the finger domain rotates toward the palm domain by 60°. As a result the

conserved basic residues in the finger domain move closer to the active site and interact with the incoming dNTP. The conformation of the thumb domain also changes upon the binding of primer–template by rotating closer to the palm domain. The thumb domain thus wraps around the primer–template DNA and makes close contact with the DNA minor groove.

A comparison of gp43 in the polymerizing mode (in the gp43–DNA–dTTP ternary structure) to the editing mode (in the gp43–DNA binary structure) provides us with a view of polymerase structural changes accompanying the switching between the two modes. The thumb domain plays an important role in the transition by holding DNA firmly with its tip. A rotation within the thumb domain between the tip and the base is thought to guide the DNA transition on a confined path between the polymerase active site and the exonuclease active site. With a 40° rotation of the double-stranded DNA, the primer terminus of the DNA travels 40 Å from the polymerase to the exonuclease active site. The structures reveal a cleft between the thumb domain and the exonuclease domain. Upon switching to the polymerizing mode, the two domains move toward each other and close the cleft.

gp45 Clamp Protein

The important function of the clamp protein in DNA replication is evident by its widespread presence in prokaryote (T4 phage and *E. coli*), eukaryote (human and yeast), and archaeon as well. The T4 gp45 crystal structure reveals a homotrimer with an inner diameter of ca. 35 Å and a thickness of ca. 25 Å (Moarefi et al. 2000). Each monomer comprises two domains that adopt a similar fold. The neighboring subunits are held together by four pairs of hydrogen bonds formed between two β-strands donated by each subunit. Although the T4 clamp has an overall negative charge, its inner surface shows positive electrostatic potentials. This unusual charge distribution favors a mechanism in which duplex DNA threads through the ring and interacts with the interior of the ring through electrostatic forces.

The high-resolution X-ray crystal structure of gp45 provided the initial view of the bacteriophage sliding clamp. To probe the clamp structure in solution, both chemical cross-linking and FRET approaches were utilized. Based on the T4 gp45 crystal structure, two unique cysteines (R86C and T167C) were introduced across the subunit interfaces by site-directed mutagenesis allowing efficient cross-linking of the neighboring subunits through disulfide bond formation. It was found that only two of the three possible disulfide bonds were formed per gp45 trimer, suggesting that one subunit interface remained open (Alley et al. 1999b). This notion was further tested by introducing two unique cysteines in the interdomain loop to form an intrasubunit cross-link. The flexibility of the interdomain loop is thought to be required for clamp opening. The separation distance across the subunit interface can be measured by introducing a FRET pair comprised of W91 and V162C-CPM (7-diethylamino-3-(4′-maleimidyl phenyl)-4-methylcoumarin). The subunit interface distance of 19 Å measured in the intrasubunit cross-linked clamp was

close to 14 Å derived from the X-ray structure of gp45, suggesting that the cross-linking of the intradomain loop facilitates the closing of the clamp. However in the absence of cross-linking the same clamp mutant demonstrated a reduced energy transfer efficiency between the FRET pair with a calculated donor–acceptor distance of ca. 38 Å. Therefore in solution the T4 clamp exists in an open conformation. Further hydrodynamic analyses of T4 gp45 corroborated this conclusion (Alley et al. 1996).

The steady-state FRET experiment may represent an average of two equilibrating states of gp45, i.e., a closed clamp and a clamp with one open interface, or alternatively a single open state. To distinguish between these two possibilities the time-resolved FRET was measured between W92 and V163C-CPM. The results indicated that gp45 exists in only one state with one open and two closed subunit interfaces (Millar et al. 2004).

Despite the low sequence identities the crystal structures of the three clamps from bacteriophage T4 (gp45), *E. coli* (β-subunit), and *S. cerevisiae* (PCNA) all form closed rings in X-ray crystal structures. However the solution structure of gp45 is unique in that it exists as an opened ring. In comparison PCNA exists as a closed ring in solution (Zhuang et al. 2006b), which is likely to be the case for the β-subunit as well. These observations agree with the differences in the oligomer stability of the three clamps with the T4 gp45 being the least stable dissociating into subunits with a K_d of 250 nM compared to the dissociation of PCNA and β-subunit (K_d ~21 nM and <60 pM, respectively) (Yao et al. 1996). An X-ray crystal structure determination of the β-subunit suggests the existence of a so-called "spring tension" in the closed ring (Jeruzalmi et al. 2001). Thus an open T4 clamp in solution is attributed to looser interactions between the trimer subunit interfaces that cannot maintain an intact ring under "tension".

An earlier study showed that a deletion of the C-terminal six amino acids of gp43 abolished the interaction between gp43 and its cognate clamp gp45 (Berdis et al. 1996). This observation suggests that gp43 interacts with gp45 through the polymerase C-terminal tail. A structural view of this notion is provided by the cocrystal structure of the RB69 gp45, which shares 78% sequence identity to the T4 gp45, bound with a gp43 C-terminal peptide (Shamoo and Steitz 1999). The binding site on gp45 is located midway between the two homologous sub-domains of the individual clamp monomer. The binding interactions are mostly hydrophobic with residues L897, M900, and F901 in the peptide bound to a hydrophobic pocket on gp45. A holoenzyme model (Fig. 16.2) that contains polymerase and clamp was built by docking the C-terminal tail of the RB69 gp43 into the known binding pocket on clamp with the guidance of a duplex DNA, which binds to the polymerase active site and at the same time threads through the interior ring of gp45. The gp43 C-terminal peptide was found to adopt different conformations in different crystals. Such flexibility in the link between gp43 and gp45 may be beneficial for processive DNA synthesis by the polymerase holoenzyme since the movement of the bound DNA between the polymerase and exonuclease sites would be well tolerated (comparing the polymerizing to the editing modes in Fig. 16.2).

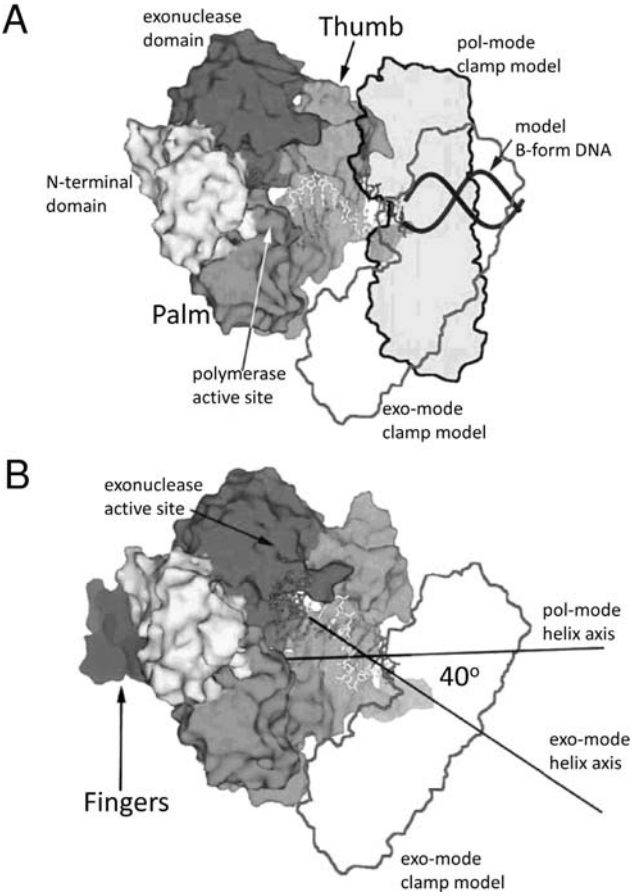

Fig. 16.2 gp43 holoenzyme model depicting the switching between polymerizing (A) and editing (B) modes. The polymerase is shown as a molecular surface model. The individual domains are labeled. The primer–template DNA in the crystal structure is shown in stick form. The modeled B-form extension of this DNA is shown as a backbone worm. The docked clamp is shown as a *black outline* to compare its position in polymerizing and editing modes. Figure adapted from (Franklin et al. 2001).

gp44/62 Clamp Loader

Loading of the clamp requires its cognate clamp loader. The T4 clamp loader is a binary complex of four gp44 subunits and one gp62 subunit. The 36 kDa gp44 subunit contains the Walker A motif and the SRC motif that are responsible for ATP binding and hydrolysis. In contrast the 21 kDa gp62 subunit contains neither motif. At present the subunit arrangement of gp44/62 complex is not clear. Nonetheless a circular structure was proposed based on analogy drawn between gp44/62 and the *E. coli* γ complex. The four gp44 subunits are thought to be equivalent to γ

and δ′ subunits in the γ complex, with the gp62 subunit equivalent to the δ subunit. Mutagenesis analysis of the *E. coli* γ complex showed that ATP hydrolysis by the clamp loader involves the SRC motif of the neighboring subunit. Since the SRC motif is absent in the gp62 subunit, one can infer that only three of the four ATP sites of gp44/62 are competent in catalyzing ATP hydrolysis if gp44/62 adopts a similar ring structure as the γ complex. Alternatively the four gp44 subunits could form a symmetric tetramer with gp62 subunit attached at an unknown site in the complex. This molecular architecture, albeit different from what is observed in the γ complex, would allow four competent ATPase sites.

The Holoenzyme Assembly Pathways

The assembly of the T4 polymerase holoenzyme requires the coordinated actions of all three holoenzyme components (gp43, gp44/62, and gp45). The order of events leading to holoenzyme formation has been investigated extensively using a combination of rapid chemical quench and stopped-flow fluorescence approaches (Alley et al. 2000; Trakselis et al. 2003a, 2001). Early efforts have focused on an assembly pathway starting with the formation of a gp44/62–gp45 binary complex in the presence of ATP. Subsequent binding of this complex to the primer–template DNA triggers the loading of gp45 onto DNA. In the last step of holoenzyme formation a physical linkage between gp43 and gp45 is established with the departure of gp44/62 from the assembled complex. Therefore gp44/62 acts as a molecular chaperon in this assembly process.

To relate ATP hydrolysis to various steps in clamp loading and subsequent holoenzyme formation, a rapid-quench technique was used to probe the fast ATP hydrolysis and to determine the stoichiometry of ATP consumption at various steps. It was found that two equivalents of ATP are hydrolyzed upon interaction with gp45 to form the gp44/62–gp45 complex. In the next step of clamp loading two more equivalents of ATP are hydrolyzed once the gp44/62–gp45 complex interacts with primer–template DNA. It should be noted that another rapid-quench experiment found one equivalent of ATP was hydrolyzed upon mixing DNA with gp44/62 and gp45 (Pietroni et al. 2001), although it was later found that the reduced ATP equivalents arise from a defect in the quenching protocol (Trakselis et al. 2003a).

Another important feature of the clamp-loading pathway is the conformational changes of gp45 catalyzed by gp44/62. To directly probe the dynamic opening and closing of gp45, the FRET signal derived from a pair of fluorophores (W92 as the donor and CPM attached to V163C as the acceptor) introduced across the clamp interface was followed using stopped-flow fluorescence (Alley et al. 2000). Upon binding to gp44/62 one gp45 subunit interface is opened further from 40 Å to greater than 45 Å as measured between W92 and V163C-CPM (note that the distance measured for W92–V163C-CPM FRET pair is larger than the distance between the closest amino acids across the open subunit) with accompanying ATP hydrolysis. Substituting ATP with ATPγS resulted in no further increase in the gp45 subunit

interface distance indicating ATP hydrolysis is required. Following the introduction of DNA to the gp44/62–gp45 binary complex, the clamp subunit interface is closed around DNA to a W92 to V163C-CPM distance of 35 Å. The DNA polymerase holoenzyme can then be formed after the addition of gp43. It has been shown that both gp44/62 and gp43 interact with the same face of the gp45 toroid (Latham et al. 1997b) and that gp44/62 departs from a gp44/62·gp43·gp45·DNA complex to form the holoenzyme (Trakselis et al. 2003a).

The opening of gp45 could be either in-plane or out-of-plane. To obtain precise information on clamp conformational changes in the various steps of clamp loading and holoenzyme formation, a total of three FRET pairs were introduced across the clamp interface to triangulate the distance changes across the subunit interfaces (Trakselis et al. 2001). Residue W92 was chosen as the fixed FRET donor, while site-specific mutations were introduced at V163C, S158C, and T168C individually to conjugate CPM as the acceptor. The stopped-flow FRET measurements revealed 10 steps in the clamp-loading process (Fig. 16.3). The distance information obtained for the individual steps was then used to derive the directionality of the gp45 opening and closing. Combined with computer modeling, the open gp45 trimer structure was constructed by adjusting the torsion angles within the interdomain loop. In state $gp45^{D}$, the clamp exists in an in-plane open conformation. Binding of DNA to the $gp45^{D}$–gp44/62 complex resulted in an initial in-plane closing of gp45 through step G followed by an out-of-plane reorientation to a spiral configuration ($gp45^{H}$). Introduction of gp43 resulted in a final in-plane closing of gp45 to an interface distance smaller than the initial distance observed for gp45 alone in solution. At this final state the interface distance remains 11 Å, consistent with accommodation of the C-terminus of gp43 within the gp45 subunit interface (Alley et al. 1999a). One can speculate that the insertion of the C-terminal peptide of gp43 to the gp45 interface can effectively relieve the "tension" incurred with a fully closed gp45 clamp.

The observation of an opened gp45 clamp in solution raised an interesting question regarding the role of gp44/62 in clamp loading and the need for ATP hydrolysis. Since gp45 is open with an interface separation large enough to allow the passage of double-strand DNA (B-form DNA has a diameter of ca. 20 Å), a question exists as to why gp44/62 is needed to further open the clamp with the consumption of two ATPs in the rapid initial steps of clamp loading. Inquiry into this question led to the discovery of an alternative pathway of gp45 loading catalyzed by gp44/62, where the clamp loader was found to bind specifically to the primer–template DNA and mark the locus of clamp loading (Zhuang et al. 2006a). This gp44/62–DNA interaction requires the hydrolysis of one equivalent of ATP to form the binary complex. Following the formation of the gp44/62–DNA complex, an open gp45 clamp is recruited to the 3′ end of the DNA primer for loading. However closing of gp45 onto DNA does not require rapid ATP hydrolysis suggesting that the electrostatic interactions between the positively charged inner rim of gp45 and the negatively charged DNA backbone likely drives the closing of gp45.

It is unique that the T4 clamp loading may occur through more than one pathway. Previous studies demonstrated that in *E. coli* and yeast the clamp could only be loaded following one pathway, i.e., the clamp loader interacts with clamp to

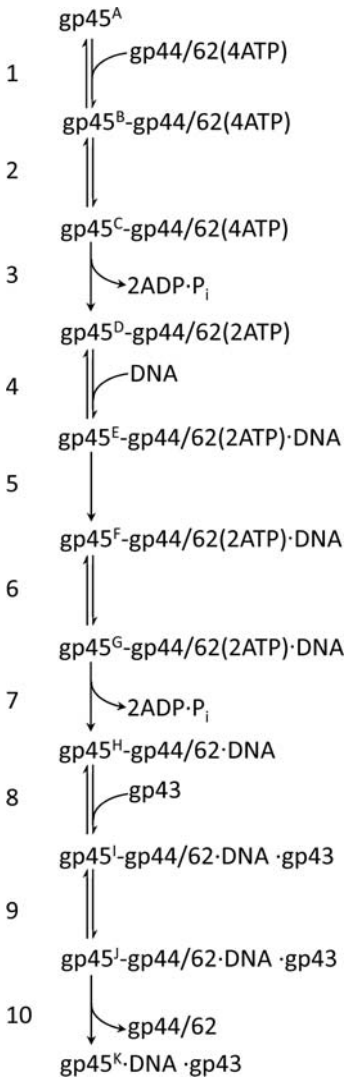

Fig. 16.3 A 10-step model depicting the holoenzyme assembly process. The different states of gp45 are designated by the superscript A through K. The equivalents of ATP bound to gp44/62 are indicated in parenthesis. See text for details.

form a binary complex, which interacts with DNA to effect the clamp loading. The difference can be understood in light of the unique solution structure of the T4 clamp and inferred from the structure of the clamp loader–clamp complex as represented by the yeast RFC–PCNA complex (Bowman et al. 2004). Five ATPase subunits of the RFC complex adopt a spiral configuration and form an inner chamber that presumably accommodates the duplex DNA. Three of the five ATPase subunits

make contact with the PCNA ring. It is evident from this structure that the initial formation of the RFC–DNA binary complex will make it topologically impossible to establish a productive interaction with PCNA, thus hindering the clamp opening. However, this may not present a problem for T4 since an opened gp45 in solution can readily encircle duplex DNA and establish interactions with the gp44/62 ATPase domains simultaneously. Therefore the open clamp conformation of T4 lends flexibility to the order of clamp loading and holoenzyme formation.

A single-molecule approach was applied to investigate in greater detail the T4 holoenzyme assembly process (Smiley et al. 2006). Individual holoenzyme components, gp43 and gp45, were labeled with fluorescent dyes Alexa Fluor 488 and 555, which are amenable for single-molecule fluorescence detection because of their high fluorescent intensity and photochemical stability. A forked DNA substrate for clamp loading was immobilized on a glass slide surface through a biotin–streptavidin interaction. The fluorescence signal from single molecules was detected with total internal reflection optics and three microscope filter sets were selected for the observation of emission from donor Alexa Fluor 488, acceptor Alexa Fluor 555 (excited at 488 and 514 nm, respectively) and emission due to FRET between the two fluorophores (excited at 488 nm). The observation of a FRET signal between labeled gp43 and gp45 suggested the close juxtaposition of holoenzyme components, accompanying the formation of the polymerase holoenzyme. The activity of the assembled holoenzyme was ensured by demonstrating strand displacement synthesis by the complex upon the addition of required deoxynucleotides. The results from these single-molecule experiments provided further support for the previously demonstrated assembly pathways and led to the discovery of additional assembly pathways including (1) gp45 binding to DNA followed by gp44/62 and then gp43 and (2) gp43 binding to DNA followed by gp44/62–gp45 complex. In all cases MgATP was required for holoenzyme assembly. The existence of the multiple holoenzyme assembly pathways revealed by in vitro experiments underscores the remarkable flexibility of the T4 holoenzyme complex, which is likely required to cope with the diverse DNA structures (D-loop, R-loop, and lagging strand DNA primed with short RNA pentamer) encountered in T4 DNA replication.

Polymerase Exchange

One salient property of the T4 DNA polymerase holoenzyme is its high processivity during DNA replication with a dissociation half-life of ca. 9 min (Yang et al. 2004). However, counterintuitively, it was demonstrated that during normal DNA replication an active exchange process takes place frequently between the gp43 in solution and the gp43 within the polymerase holoenzyme (Yang et al. 2004). Given an estimated in vivo gp43 concentration of ca. 600 nM the polymerase exchange on any given replisome would occur on average once every 10 s, or approximately 90 events per replication fork during the 15 min time span for copying the T4 genome.

A model for the T4 polymerase exchange process was proposed based on molecular modeling using the available X-ray crystal structures of gp45 and RB69 gp43

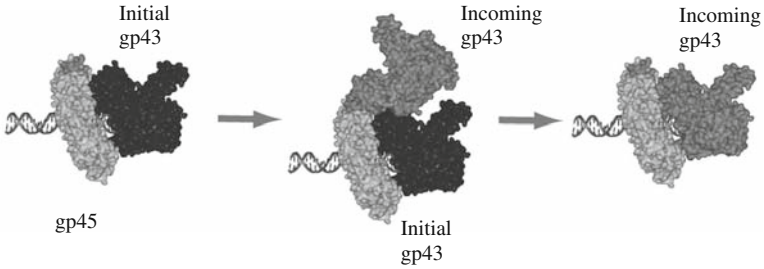

Fig. 16.4 Solution structure models of polymerase exchange. The clamp protein gp45 is shown as a toroid encircling DNA. The initial and incoming polymerases gp43 are both depicted as molecular surface models.

(Fig. 16.4). In this model, gp45 acts as a platform for the exchange process. The incoming polymerase likely binds to a second polymerase-binding site on gp45 to avoid a steric clash with the resident gp43. Given the frequency of stalling of the DNA replisome, the polymerase exchange process uncovered for the T4 polymerase holoenzyme may serve to overcome the replication barriers. Given that the clamp-polymerase structure and interaction appears to be widely conserved across all three branches of life, the polymerase exchange property observed for T4 may be applicable to other replication systems.

gp32 ssDNA-Binding Protein

The T4 phage ssDNA-binding protein (gp32, 301 a.a.) is considered to be a prototype for ssDNA-binding proteins. gp32 is absolutely required for DNA replication in vivo (Curtis and Alberts 1976) and reconstitution of coupled leading and lagging strand DNA synthesis in vitro (Huberman et al. 1971; Yang et al. 2003). Additionally, gp32 is required for homologous recombination, DNA repair, transcription, and DNA packaging (Miller et al. 2003). The binding of gp32 to ssDNA is very tight ($K_d = 0.1\ \mu M$ on long ssDNA strands), highly cooperative, and sequence non-specific (Kelly et al. 1976). The binding site size has been determined to be 7–9 bases of ssDNA and the cooperativity parameter (ω) is greater than 1000 (Kowalczykowski et al. 1980). gp32 contains three distinct domains, which were initially isolated and characterized using limited proteolysis. The N-terminal domain (referred to as domain B for "basic") is involved in cooperative ssDNA binding, such that removal of residues 1–21 completely eliminates binding cooperativity (Giedroc et al. 1990). The major function of the highly acidic C-terminal domain (residues 254–301, referred to as domain A for "acidic") is to interact with other T4 proteins. Affinity chromatography using gp32-agarose has detected interactions between gp32 and itself, gp43, gp45, and gp59 (Formosa et al. 1983; Morrical et al. 1996). gp32 also has been shown to co-purify with gp61 (Burke et al. 1985). The structure of the gp32 core domain (residues 22–253) in complex with a six-base

ssDNA oligonucleotide has been solved using X-ray crystallography (Shamoo et al. 1995). The core domain contains the ssDNA-binding site and is made up of three smaller sub-domains. The sub-domains are (1) a zinc-finger motif that is thought to be important for protein stability; (2) a five-stranded β-sheet containing several aromatic side chains involved in DNA base recognition; and (3) a connecting region bridging sub-domains 1 and 2. The affinity of the core domain for short ssDNA oligos (which can only accommodate a single gp32 monomer) is essentially identical to that of the full-length protein. However, due to the loss of cooperative interactions, the affinity of the core domain for long ssDNA strands is greatly reduced compared to the full-length protein (Giedroc et al. 1990).

gp59 Helicase-Loading Protein

gp59 helicase-loading protein (gp59, 217 a.a) is a basic protein that plays a central role in the assembly and possibly the function of the T4 phage replisome. In vivo, gp59 is necessary for recombination-dependent initiation of replication and gp59 mutants display the classic DNA arrest phenotype that is indicative of that defect (Wu and Yeh 1975; Dudas and Kreuzer 2005). gp59 was first isolated and described as a helicase assembly protein by the Alberts laboratory (Barry and Alberts 1994), making it the final member to the eight protein set that makes up the T4 replisome (Barry and Alberts 1994).

Equilibrium fluorescence and gel mobility shift experiments have demonstrated that gp59 binds to a variety of ss and dsDNA substrates in a sequence-independent fashion (Lefebvre and Morrical 1997; Mueser et al. 2000; Jones et al. 2000). However, gp59 shows a distinct preference for forked DNA structures over substrates that contain only ssDNA or dsDNA (Jones et al. 2000). These preferred structures are D-loops, R-loops, three- and four-stranded Holliday junctions, and model replication forks (Nelson et al. 2006; Nossal et al. 2001). When binding to a model replication fork, gp59 requires at least six bases of ssDNA before the ss/ds junction (Jones et al. 2000). This is consistent with the number of single-strand DNA bases bound by the gp59 monomer as determined by fluorescence enhancement of etheno-modified ssDNA (Lefebvre and Morrical 1997).

The oligomeric state of the functional form of gp59 is unclear. Kinetic evidence indicates that a 1:1 ratio of gp59 to gp41 subunits (which is hexameric) provides the maximal enhancement of gp41 loading (Raney et al. 1996). Additionally, cross-linking studies have shown that gp59 can induce the oligomerization of gp41 and that gp59 forms up to pentamers in the presence of DNA or gp32 (Ishmael et al. 2002, 2001). Together, these data suggest that gp59 may be hexameric at the replication fork. On the other hand, sedimentation velocity and glycerol gradient centrifugation experiments have shown that gp59 in solution is monomeric in the absence of DNA substrate (Yonesaki 1994; Xu et al. 2001).

The structure of gp59 was determined in the Nossal and Mueser laboratories (gp59 subunit of Figs. 16.5 and 16.6; Mueser et al. 2000). gp59 is essentially an alpha-helical protein with two domains, the N-domain (residues 1–109) and the

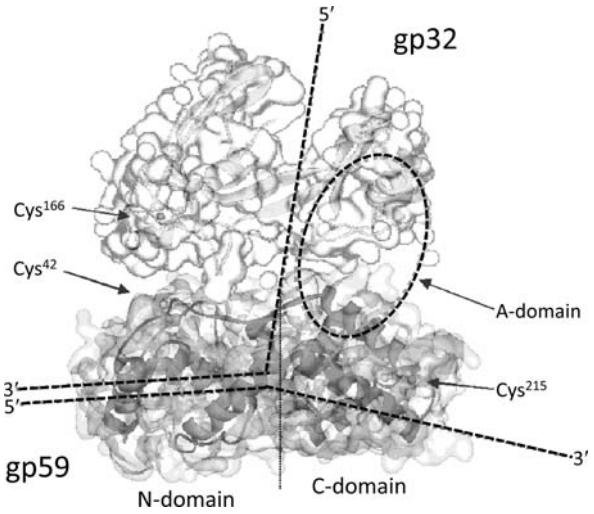

Fig. 16.5 Model of the gp32–gp59 complex. gp59 is predicted to associate with the replication fork such that the N-terminal domain binds to the duplex and the lagging strand traverses a groove between the N- and C-terminal domains (Mueser et al. 2000). This orientation of gp59 on DNA places Cys-42 in close contact with Cys-166 of gp32, which is bound to ssDNA. The A-domain of gp32 most likely interacts with the C-terminal domain of gp59. Figure adapted from (Ishmael et al. 2001).

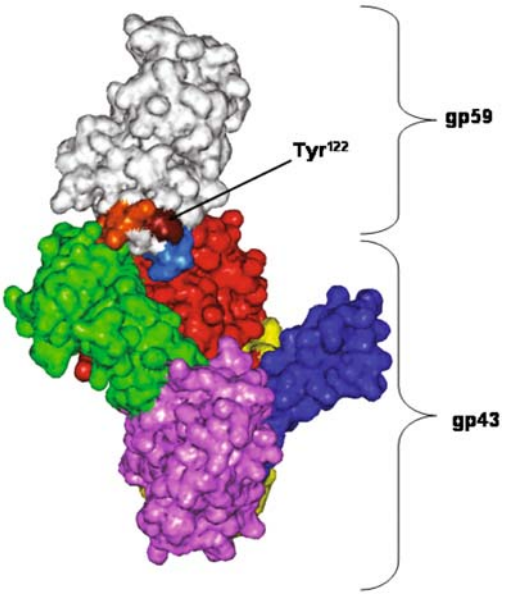

Fig. 16.6 Interaction model of the gp43–gp59 complex. The proposed interaction model (Xi et al. 2005a) showing the location of Y122A near the interface between gp43 and gp59. The N-terminal, exonuclease, palm, fingers, and thumb domains of gp43 are colored as *yellow*, *red*, *magenta*, *blue*, and *green*, respectively. gp59 is colored *gray* except for residue Y122 (*maroon*), N202-K217 (*cyan*), and K126 to E134 (*gold*).

C-domain (residues 110–217). A portion (residues 9–65) of the N-domain shows structural similarity to members of the high-mobility-group (HMG) family of DNA minor groove-binding proteins. Based on this structural similarity a speculative model for the interaction of monomeric gp59 with the ss/ds junction of a replication fork has been proposed (Mueser et al. 2000). The HMG region of gp59 is postulated to bind at the duplex region ahead of the fork in much the same manner as HMG1 binds to the fork region of a four-stranded Holliday junction (Hardman et al. 1995). The ssDNA that would make up the lagging strand arm behind the fork binds in a shallow groove located in the junction between the N- and C-domains of the protein and a hydrophobic region on the surface of the C-domain interacts with the other ssDNA arm (leading strand) behind the replication fork. Site-specific mutants designed to test this model have revealed a single residue, I87, that when mutated reduces the affinity of gp59 for both forked and single-stranded DNA (Jones et al. 2004a). In the proposed model for the interaction of gp59 with fDNA, I87 is positioned at the site where the ssDNA arms begin to separate from the duplex (fork region). The other mutations that were located in the duplex region, leading strand arm, and lagging strand arm had little effect on the affinity for forked DNA structures. It is possible that the loss of a single interaction point, except for those located precisely in the fork region, does not cause a loss of binding affinity great enough to be detected in gel mobility shift experiments or alternatively, the proposed model does not accurately reflect the gp59–fDNA structure given the possibility that gp59 is in a higher order oligomeric state when bound to fDNA.

gp41 Helicase

Helicases, like the T4 phage helicase (gp41, 475 a.a.), are enzymes that play an essential role in nearly all DNA metabolic processes, catalyzing the transient opening of DNA duplexes. Mutations in gene 41 strongly reduce the amount of DNA replication in phage-infected cells (Epstein et al. 1963) and eliminate synthesis on the lagging strand (Kreuzer and Morrical 1994). The purified gp41 exhibits a DNA-dependent ATPase or GTPase activity, which is strongly stimulated by long pieces of ssDNA rather than short pieces of ssDNA or dsDNA (Liu and Alberts 1981a). Nucleotide hydrolysis powers DNA unwinding by gp41 (Venkatesan et al. 1982) or translocation of gp41 on ssDNA (Young et al. 1994) in a unidirectional 5′-to-3′ manner. The preferred DNA substrates of gp41 are preformed forked DNA hybrids with an absolute requirement for a 5′-ssDNA tail of 32 nt or more (Venkatesan et al. 1982). Optimal DNA unwinding also requires a 3′-ssDNA extension longer than 29 nt suggesting that the gp41 protein interacts with both the leading strand and lagging strand templates at the replication fork as it unwinds the duplex region (Richardson and Nossal 1989). The length of the 5′-ssDNA tail and the necessity for the 3′-ssDNA tail are reduced in the presence of gp59 (Jones et al. 2000; Yonesaki 1994). Nucleotide triphosphate binding, but not hydrolysis, is necessary for stable gp41–ssDNA complex formation (Liu and Alberts 1981a; Richardson and Nossal 1989). A binding site size of 12–20 nt per gp41 monomer has been determined

by electrophoretic mobility shift assays with gp41 and $dT_{12–20}$ in the presence of nucleotide (Young et al. 1994).

The gp41 protein alone will translocate on ssDNA at a rate of 400 nt/s with an association half-life of 1 min (Liu and Alberts 1981a). The DNA unwinding rate of gp41, measured at 30 bp/s in the presence of gp59 (Raney et al. 1996), and the processivity of unwinding (ca. 650 nt) in the presence of gp61 on long duplexes (Richardson and Nossal 1989) are much lower. However, the gp41 protein alone is necessary and sufficient to establish a high processive rate (∼250 bp/s) of unwinding during DNA synthesis on the leading strand by the polymerase holoenzyme (Alberts et al. 1980; Cha and Alberts 1989). In a complete replisome, a dissociation half-life for gp41 of 11 min was measured by dilution experiments, revealing that the 41 protein is sufficiently processive to finish replicating the entire T4 genome (168 kb) at the observed replication rate of ∼400 nt/s (Schrock and Alberts 1996).

The oligomerization of gp41 has been observed by numerous groups using a variety of techniques. Oligomerization of gp41 was first reported by Liu and Alberts (1981a) who detected a sigmoidal dependence of nucleotide hydrolysis on gp41 concentration and an increased sedimentation rate with GTPγS in sucrose gradients. Further studies have shown that gp41 exists as a monomer/dimer equilibrium when free in solution (primarily as a dimer at physiological protein concentrations) and forms a hexamer upon activation by ATP or ATPγS binding with the assembly of dimers to tetramers to hexamers (Dong et al. 1995). Cryoelectron microscopy (Dong et al. 1995) and protein cross-linking (Morris and Raney 1999) suggest these hexamers are toroidal rings with ssDNA probably passing through the center like other hexameric helicases (Stasiak et al. 1994; Egelman et al. 1995). The most recent electron microscopy of gp41 reveals two distinct forms of gp41 hexamers, termed "open" and "closed", which may be important for the assembly of gp41 onto ssDNA (Norcum et al. 2005).

gp61 Primase

The T4 phage primase protein (gp61, 342 a.a.) is essential for normal DNA synthesis in vivo. T4 phage defective in gene 61 has a reduced rate of DNA synthesis (Yegian et al. 1971) and accumulates abnormal amounts of ssDNA (Gold et al. 1976). gp61 catalyzes the synthesis of short RNA molecules used as primers for DNA polymerase on the lagging strand of a replication fork. The in vivo recognition site for priming is 5′-GTT-3′, additionally 5′-GCT-3′ can be used in vitro. Although the 3′-T is required for recognition, it is not copied into the resulting primer; the primers therefore have the sequence 5′-pppACNNN-3′ and 5′-pppGCNNN-3′, respectively (Cha and Alberts 1986). High concentrations of gp61 alone synthesize primers, mostly dimers and a small number of primers 5–45 nt long, mainly from the 5′-GCT-3′ priming site (Cha and Alberts 1986; Hinton and Nossal 1987). The combination of gp41 and gp61 greatly increases the overall primer synthesis rate favoring a pentaribonucleotide product over the dimer and the use of the 5′-GTT-3′ rather than the 5′-GCT-3′ recognition site (Hinton and Nossal 1987; Cha and Alberts

1990). Including optimal levels of gp32, gp59, and gp41 have produced a priming rate of almost one primer per second per primosome, a rate sufficient for the in vivo operation of the replisome (Valentine et al. 2001).

Similar to other prokaryotic primase proteins, gp61 is made up of three domains. The N-terminal domain contains a zinc-binding domain known as a zinc ribbon. The single zinc ion is bound by residues C37, C40, C65, and C68 (Valentine et al. 2001). When the zinc ribbon sequence in the T7 primase was replaced with those from *E. coli* and T4, the resulting chimeric proteins were active but primed at sequences different than either of the parent proteins (Kusakabe and Richardson 1996), strongly suggesting that some, but not all, of the priming site recognition is afforded by the zinc ribbon motif. The middle domain of the primase is the catalytic domain, responsible for ribonucleotide polymerization and the C-terminal domain is involved in protein–protein interactions with the helicase (Jing et al. 1999).

Analytical ultracentrifugation or isothermal titration calorimetry (ITC) displayed no evidence for primase self-association suggesting that gp61 alone in solution is monomeric (Valentine et al. 2001). In the presence of DNA and/or gp41, a study using gel mobility shift analysis suggested a monomeric primase as the active component of the primosome (Dong and von Hippel 1996). However, in more recent investigations, gp61 has been observed to bind to short ssDNA oligos primarily as a trimer by ITC and chemical cross-linking techniques (Valentine et al. 2001) and as a hexamer by fluorescence anisotropy with dye-labeled ssDNA with a K_d of 50–100 nM (Yang et al. 2005). Furthermore, a three-dimensional reconstruction from electron microscopic images indicates a ring-like structure and a hexameric stoichiometry for gp61 when complexed with ssDNA (Norcum et al. 2005). Defective primases either missing the N-terminal zinc-binding domain (deletion mutant) or full-length catalytically inactive (active site mutant) proteins without priming activity could be mixed to create oligomeric primases with restored catalytic activity suggesting that oligomers of gp61 may also be functional.

Interaction Between gp32 and gp59

The initial characterization of gp59 established its role as an accessory protein required for the loading of the gp41 helicase onto gp32-coated ssDNA (Barry and Alberts 1994; Morrical et al. 1994). gp59-agarose affinity chromatography also indicated that gp32 and gp59 interact with each other (Yonesaki 1994). Based on these and other data it was proposed that a direct interaction between gp59 and gp32 facilitated the loading of gp41 helicase onto DNA (Barry and Alberts 1994). Since those initial observations, the interaction between gp32 and gp59 has been extensively characterized using a wide variety of techniques such as protein cross-linking, ensemble and single-molecule FRET, analytical ultracentrifugation, and in vitro replication kinetic assays.

Thiol–thiol cross-linking has been used to identify the specific points of interaction between gp32 and gp59 (Ishmael et al. 2001). It was found that C166 on gp32 and C42 on gp59 must be within 6 Å of each other. These experiments also revealed

higher order oligomeric states of gp59. In the presence of either ssDNA or gp32, species of gp59 that ranged up to a pentameric subunit composition were observed. Further experiments showed that the A-domain of gp32 is required for this gp32-induced gp59 oligomerization. However, while the A-domain greatly increases the interaction between gp32 and gp59, it is not absolutely required. Based on these cross-linking results, the model of the gp59–fDNA complex (Mueser et al. 2000) was expanded to include gp32 (Fig. 16.5). Here, gp32 is bound to the lagging strand ssDNA and interacts with gp59 at both its N- and C-domains. The gp32 core domain, which contains C166, makes contact with the N-domain of gp59, whereas the gp32 A-domain interacts with the C-domain.

While protein cross-linking experiments are highly informative with regard to the specific sites of interactions between two proteins, fluorescent experiments are better suited for the determination of stoichiometry and binding affinities. Labeling of gp59 at C42 with the fluorescent dye rhodamine has allowed the anisotropy of gp59 and gp59 in complex with gp32 truncation mutants to be monitored (full-length gp32 was not tested due to insolubility problems) (Xu et al. 2001). Both gp32-B (gp32 missing the N-terminal B domain) and gp32A (only the A-domain) bind gp59 with a 1:1 stoichiometry (Xu et al. 2001). The K_d for the interaction of gp59-rhodamine with gp32-B and gp32A are 10 and 3 nM, respectively. In addition to fluorescent anisotropy, ensemble FRET experiments have found a 1:1 stoichiometry between gp59 and gp32 on both single-stranded and forked DNA substrates (Zhang et al. 2005) and the Morrical lab has used etheno-modified ssDNA to demonstrate that gp59 and gp32 simultaneously co-occupy ssDNA (Lefebvre et al. 1999).

Reconstitution of replisome-mediated DNA synthesis has revealed the necessity of the gp32–gp59 complex for productive loading of gp41 helicase (Jones et al. 2004b; Ma et al. 2004). Consequently, when gp59 loads gp41 onto a replication fork, an interaction between gp32 and gp59 must occur. If gp41 loads without the aid of gp59, the presence of gp32 is not required (Jones et al. 2004b). Mutational analysis of gp32 indicates that the ability of gp32 to bind both gp59 and ssDNA is necessary for this effect (Ma et al. 2004). Based on these results and others, the Morrical lab has proposed that a gp59–gp32 cluster (presumably in a 6:6 ratio) forms a condensed-coil structure termed the helicase-loading complex (HLC). The HLC recruits gp41 dimers that form hexamers at the fork and is proposed to slide along ssDNA, thus allowing it to remain with a moving replication fork (Ma et al. 2004).

Interaction Between gp43 and gp59

Almost immediately after gp59 was discovered, it was found that high concentrations of gp59 inhibited both helicase-dependent and helicase-independent DNA synthesis in vitro (Barry and Alberts 1994). Strong inhibition of replication was also observed in vivo when gp59 was over-expressed from an IPTG-inducible plasmid (Spacciapoli and Nossal 1994). More recently, gp59 was shown to inhibit in vitro

replication when initiating from an R-loop in the absence of gp41 helicase (Nossal et al. 2001). Several possible explanations for the inhibition of DNA synthesis by gp59 have been proposed, such as acting as a steric block, sequestering protein off DNA, and interacting directly with a component of the replisome. The latter has been proven to be correct.

A site-specific cross-link has been observed between gp59 and gp43 polymerase in the presence of a forked DNA substrate and was confirmed using FRET experiments (Ishmael et al. 2003). gp43 polymerase was labeled N-terminally with Oregon Green dye and gp59 was labeled at C42 with CPM dye. When the two labeled proteins were mixed in the presence of forked DNA, a small but significant amount of energy transfer was observed (Ishmael et al. 2003; Xi et al. 2005a). The data from these two complementary experiments clearly demonstrate an interaction between gp43 and gp59. Further experiments were done to map the site of interaction between gp43 and gp59 (Xi et al. 2005a). The cross-linked protein was subjected to in-gel digestion followed by MALDI-TOF mass spectrometry. A unique fragment was identified and the site of interaction was determined to be C215 of gp59 and C169 of gp43. This information, coupled with FRET distance measurements, was used to evaluate the top 30 models from a series of computer-generated (ClusPro) interaction models for the gp43–gp59 complex (Xi et al. 2005a). The first constraint applied was that gp59-C215 and gp43-C169 must be within 10.2 Å of each other (the length of the cross-linker). The second constraint was that gp59-C42 and the N-terminus of gp43 must be about 50 Å apart (based on FRET efficiency). These two constraints reduced the number of possible models from 30 to 1 (Fig. 16.6). In this model gp59-C215 and gp43-C169 are 8 Å apart and gp59-C42 and the N-terminus of gp43 are located 55 Å apart. The interaction model rationalizes the inhibition of gp43 by gp59. The C-terminal helix of gp59 is inserted into a cleft between the thumb and exonuclease domains of gp43. Presumably, this insertion prevents the closing of the cleft and therefore interferes with the switching of the polymerase from its exonuclease to polymerase modes. As predicted from this model, gp59 inhibits both the polymerase activity and the exonuclease activity of gp43 (Xi et al. 2005a; Nelson et al. 2006). This result also demonstrates that gp59 is not merely acting as a block impeding the forward movement of the polymerase, but it forms a discrete complex with gp43 and inhibits both forward and backward movements by a direct interaction.

In a mutational screen for putative protein–protein interaction hotspots located on the surface of gp59, a single mutation Y122A was found to have drastically altered properties compared to the wild-type enzyme (Nelson et al. 2006). The defect most relevant to the interaction model is that Y122A is unable to inhibit the exonuclease activity of gp43. Additional FRET experiments similar to those described above indicated that the interaction between gp59 and gp43 was disrupted by the mutation. The interaction model of the gp59–gp43 complex places Y122 directly between two regions (helix H7 and loop H6–H7) of gp59 that are predicted to interact with gp43 (Fig. 16.6). Based on this central location, the role of Y122 may be to stabilize helix H13 of gp43 and the loop H6–H7 of gp59 in their interactions with gp43. This

explanation is strengthened by the fact that helix H7 of gp59, which contains Y122, makes extensive contacts with both helix H6 and H13 of gp43.

A thorough study of the in vivo effects of gp59 deficiency has revealed a physiological function of gp43 inhibition by gp59 (Dudas and Kreuzer 2005). In both the presence and absence of gp59, DNA replication that initiates from R-loop-containing origins occurs with coupled leading and lagging strand DNA synthesis. After a short delay, a second replication fork with opposite directionality to the first (retrograde synthesis) is initiated. In wild-type cells, retrograde replication occurs in a similar fashion as the first replication fork with coupled leading and lagging strand DNA synthesis. However, in the absence of gp59, lagging strand synthesis does not occur in the retrograde replication fork. Based on these results, a model in which gp59 inhibits the leading strand polymerase until the helicase and primase are loaded onto the leading strand template was proposed (Dudas and Kreuzer 2005). This is in complete agreement with the model based on in vitro data (Xi et al. 2005a).

Interaction Between gp59 and gp41

The primary function of gp59 is to load gp41 helicase onto the lagging strand DNA template, therefore a large number of studies have documented the functional interaction between gp41 and gp59. This section will focus on the direct physical interaction between the two proteins.

The architecture of the gp41–gp59 complex both on and off DNA has been studied using protein cross-linking (Ishmael et al. 2002). A cysteine residue was added to the C-terminus of gp41 by cleavage of a gp41–intein fusion with cysteine. This cysteine residue was then modified with a photoactivable cross-linker and incubated with gp59 under UV light. It was found that the C-terminus of gp41 and gp59 is in close proximity in the presence and absence of ATP and with or without DNA substrate. A similar experiment was performed with gp41 labeled at its N-terminus with a photoactivable cross-linker. With the cross-linker in this position, the N-terminus of gp41 cross-linked to gp59 both on and off DNA in the presence and absence of ATP. Next, thiol–thiol cross-linking revealed that the C-terminus of gp41 is in close proximity to C215 of gp59 in the presence or absence of ATP. However, when DNA was included in the cross-linking reaction, no cross-link between gp41 and gp59 was observed. When coupled with the previous result demonstrating that gp41 and gp59 do indeed interact on DNA, this result indicates that a conformational change occurs when the gp41–gp59 complex binds to the replication fork. Defining the exact nature of this conformational change will require a high-resolution structure of the gp59–gp41 complex.

As discussed above, gp59 inhibits the polymerase and exonuclease activities of gp43 through a direct protein–protein interaction (Xi et al. 2005a). This specific interaction has been observed using single-molecule FRET (Xi et al. 2005a,b). It was found that addition of gp41 and ATP to the gp43–gp59–fDNA complex results in the release of gp59 from the replication fork. Ensemble studies indicate that the

polymerase is "unlocked" from its gp43–gp59 interaction and is capable of DNA synthesis following the displacement of gp59 by gp41. The gp43–gp59 complex was not disrupted when gp41 was loaded in the presence of the non-hydrolyzable analog ATPγS, suggesting that translocation by gp41 is necessary for the effect. The fate of gp59 following displacement by gp41 is still unclear. Several studies using small model substrates indicate that gp59 is released into solution following displacement by gp41; however, electron microscopy studies using larger DNA substrates indicate that gp59 remains behind the replication fork in complex with gp32 on the ssDNA of the lagging strand template (Chastain et al. 2003). The effect of this complex on the replication fork appears to be minimal (if any) since once the replisome is assembled, leading and lagging strand synthesis is unaffected by the absence of gp59 (Xi et al. 2005b).

Interaction Between gp41 and gp61

When first identified and isolated, it was unclear which protein, gp41 or gp61, was the T4 helicase or primase and whether they only had activity as a complex (Nossal 1980; Liu and Alberts 1980, 1981b). It was not until higher protein amounts were obtained that we learned each protein had a different activity and that they could function independent of one another. However, their activities remain closely associated since the unwinding rate and processivity of gp41 are increased in the presence of gp61. Also, gp41 greatly increases the overall priming rate and influences the sequence of primers made by gp61. A gp41–gp61 complex on ssDNA, which requires nucleotide binding to form, has been detected by electrophoretic mobility shift assays (Richardson and Nossal 1989; Jing, Beechem and Patton 2004) and by single-molecule FRET studies (Zhang et al. 2005). The interaction between gp41 and gp61 as measured by isothermal titration calorimetry is 10-fold stronger on ssDNA than in solution (Valentine et al. 2001). Protein kinase protection experiments with gp61 tagged with a phosphorylation sequence at either the N- or C-terminus have demonstrated that the N-terminal domain of primase is protected from phosphorylation by binding ssDNA, both the N- and C-terminus are equally protected when complexed with gp41, and almost no phosphorylation occurs in the ternary complex of gp61, gp41, and ssDNA (Jing et al. 1999). Despite all this evidence, a gp41–gp61 complex has not been isolated to date.

Summary of Replisome Assembly

Based on all the available evidence, a likely (although speculative) pathway for T4 phage replisome assembly is described. We have chosen to describe assembly at a D-loop since the majority of T4 DNA replication originates from this type of structure (Kreuzer 2000). Immediately after D-loop formation, gp32 coats the displaced ssDNA and recruits gp59 monomers to the fork region of the D-loop. The exact number of gp59 monomers is dependent on the length of the displaced

strand and the number of bound gp32 monomers. Several (presumably six) of the gp32–gp59 complexes nearest the fork condense to form the coiled helicase-loading complex (HLC). Next, the clamp loader in complex with a clamp protein binds to the ss/dsDNA junction and the clamp loader chaperones the loading of the clamp onto the dsDNA. The holoenzyme is formed when the polymerase binds to the clamp protein and displaces the clamp loader from the complex. As noted above, there are several possible pathways for holoenzyme assembly and the one given here is not necessarily dominant. At this stage, the progression of the holoenzyme is prevented through a direct interaction between a gp59 monomer and the polymerase. Following holoenzyme formation, gp41 dimers are recruited to the replication fork by the HLC and each dimer forms an interaction with two gp59 monomers. Before hexameric helicase can form, the single gp59 monomer that is in complex with the polymerase must break its interaction with the polymerase and form a new interaction with gp41. Once all gp59 monomers are in complex with gp41, gp41 is fully loaded and translocation begins with ATP hydrolysis. ATP hydrolysis by gp41 either displaces gp59 from the replication fork or gp59 slides behind the fork onto the ssDNA. Leading strand replication begins immediately after the gp59–gp43 interaction is broken and gp41 begins to unwind the DNA duplex. Lagging strand replication is initiated when gp61 binds to gp41 helicase and begins to synthesize RNA pentamers on the lagging strand template. Finally, the lagging strand holoenzyme is formed at the RNA primer and lagging strand DNA synthesis proceeds. At this point, replisome assembly is complete and coordinated leading and lagging strand replication begins.

Coordination of Leading and Lagging Strand Synthesis

Once the replisome is assembled, the individual proteins act in concert to simultaneously replicate both strands of the DNA duplex. During replication the replisome undergoes a repeated remodeling process where specific proteins enter and exit the replisome as the replication fork travels down the DNA duplex. Dilution and protein trapping experiments indicate that the clamp, clamp loader, primase, and gp32 proteins dissociate from the actively replicating replisome and exchange with proteins in solution before returning to the replication fork (Kadyrov and Drake 2001; Trakselis et al. 2003b). Similar experiments have demonstrated the processivity of the helicase and both of the leading and lagging strand polymerases (Alberts et al. 1983; Yang et al. 2004). The half-life of the helicase and polymerases are on the order of several minutes, which enables complete replication of the 168 kb phage genome (Kaboord and Benkovic 1993; Yang et al. 2004).

Because of the high processivity of the lagging strand polymerase, coupled with its 5′ to 3′ direction of DNA synthesis, one problem faced by all DNA replication machineries is how to simultaneously and coordinately replicate two antiparallel DNA strands. The major hypothesis put forth to reconcile this problem is that the replisome and replication fork form a specific structure so that the two holoenzyme complexes are in close proximity to each other and the lagging strand DNA template is folded

back to form a loop (see Fig. 16.1). This enables both polymerases to synthesize DNA in the 5′ to 3′ direction while allowing the replication fork to move in the same direction (Alberts et al. 1983). The lagging strand loop that is predicted by the trombone model has been directly visualized using electron microscopy (Chastain et al. 2000). Although the lagging strand polymerase is processive, lagging strand DNA synthesis is discontinuous and results in short Okazaki fragments with an average length of 1–2 kb (Chastain et al. 2000). This discontinuous yet processive synthesis requires a specific mechanism for the release of the lagging strand polymerase from its template and its recycling to the newly synthesized pentameric RNA primer. Several mechanisms have been proposed to serve as the trigger for the release and recycling of the lagging strand polymerase. Among them, two mechanisms have gained the most experimental support. In the first model (the collision model), RNA primer synthesis and lagging strand holoenzyme release and recycling is triggered by the collision of the lagging strand polymerase into the end of the previous Okazaki fragment (Alberts et al. 1983). In support of this model, the off rate of the holoenzyme is greatly increased by a hairpin structure (Hacker and Alberts 1994) or an annealed DNA or RNA designed to mimic the 5′-end of the previous Okazaki fragment (Carver et al. 1997). In the second model (signaling model), lagging strand polymerase releases and recycles as the result of distinct macromolecular interaction events involved in repetitive lagging strand cycles, such as the association of the primase with the replisome, the RNA primer synthesis, or the loading of the clamp onto the newly synthesized primer (Wu et al. 1992). Recently, evidence for this model has come from a study demonstrating that under conditions that slow the lagging strand polymerase relative to the leading strand polymerase ssDNA gaps form between Okazaki fragments (Yang et al. 2006). The existence of gaps between successive Okazaki fragments cannot be accommodated within the confines of the collision model. In order for ssDNA gaps to form, the lagging strand polymerase must release and recycle prior to reaching the 5′-end of the previous Okazaki fragment. The nature of the signal for this release is still unclear. However, the modulation of RNA primer utilization and Okazaki fragment size by clamp and clamp loader concentrations may indicate that the loading of the clamp onto the newly synthesized RNA primer signals lagging strand polymerase recycling (Yang et al. 2006). Due to the stochastic nature of the recycling signal, in some cases the polymerase will reach the end of the lagging strand template before the signal is sent. In these situations, the polymerase may release and recycle via the collision mechanism.

The signaling model as presented above requires that the transfer of the RNA primer to the lagging strand polymerase from the primase occurs via the clamp and clamp loader. This is reminiscent of the indirect primer transfer mechanism that is well documented in the *E. coli* replication system (Yuzhakov et al. 1999). However, in the T4 phage system, solid evidence supporting the indirect transfer of the RNA primer to the lagging strand polymerase is lacking, as it is only inferred from the signaling model. Additionally, since the collision mechanism of lagging strand polymerase release and recycling may also occur, a direct transfer of the primer to the polymerase (before clamp loading) may be possible in these situations (Kato et al. 2001).

Future Directions

The T4 replisome has been proven to be an invaluable system for studying the molecular mechanism of DNA replication. We expect it will continue to provide useful new information. Several prominent questions regarding DNA replication in general can be addressed using the reconstituted T4 replisome as a model system. Central to efficient DNA replication is the coordinated DNA synthesis in both leading and lagging strands. More challenges lie in the understanding of the discontinuous lagging strand DNA synthesis. One prominent question is how lagging strand DNA polymerase is disengaged from the ongoing Okazaki fragment synthesis and initiates the next round of lagging strand synthesis. Future studies should shed light on what drives the gymnastic movement of the DNA polymerase in the lagging strand milieu. At present, most attention has been focused on the protein portion of the T4 replisome. It will be equally important to obtain a more precise picture of the DNA configuration at the replication fork, for example, how DNA threads through the protein complexes, especially the primosome. The DNA within the replisome is likely to be highly dynamic and the understanding of its movement in a confined space is crucial to our understanding of the lagging strand recycling process. Another challenge is to study the replication process in vivo with the recent advance of fluorescent approaches that make it possible to image single proteins or single complexes with high temporal and spatial resolution in live cells.

References

Alberts, B. M., Barry, J., Bedinger, P., Burke, R. L., Hibner, U., Liu, C.-C., and Sheridian, R. 1980. In Mechanistic Studies of DNA replication and Genetic Recombination, ed. B. M. Alberts, pp. 449–471. New York: Academic Press

Alberts, B. M., Barry, J., Bedinger, P., Formosa, T., Jongeneel, C. V., and Kreuzer, K. N. 1983. Studies on DNA replication in the bacteriophage T4 in vitro system. Cold Spring Harb. Symp. Quant. Biol. 47:655–668.

Alley, S. C., Jones, A. D., Soumillion, P., and Benkovic, S. J. 1999a. The carboxyl terminus of the bacteriophage T4 DNA polymerase contacts its sliding clamp at the subunit interface. J. Biol. Chem. 274:24485–24489.

Alley, S. C., Shier, V. K., Abel-Santos, E., Sexton, D. J., Soumillion, P., and Benkovic, S. J. 1999b. Sliding clamp of the bacteriophage T4 polymerase has open and closed subunit interfaces in solution. Biochemistry 38:7696–7709.

Alley, S. C., Abel-Santos, E., and Benkovic, S. J. 2000. Tracking sliding clamp opening and closing during bacteriophage T4 DNA polymerase holoenzyme assembly. Biochemistry 39:3076–3090.

Barry, J., and Alberts, B. 1994. Purification and characterization of bacteriophage T4 gene 59 protein. A DNA helicase assembly protein involved in DNA replication. J. Biol. Chem. 269:33049–33062.

Berdis, A. J., Soumillion, P., and Benkovic, S. J. 1996. The carboxyl terminus of the bacteriophage T4 DNA polymerase is required for holoenzyme complex formation. Proc. Natl. Acad. Sci. USA 93:12822–12827.

Bowman, G. D., O′Donnell, M., and Kuriyan, J. 2004. Structural analysis of a eukaryotic sliding DNA clamp-clamp loader complex. Nature 429:724–730.

Burke, R. L., Munn, M., Barry, J., and Alberts, B. M. 1985. Purification and properties of the bacteriophage T4 gene 61 RNA priming protein. J. Biol. Chem. 260:1711–1722.

Carver, T. E. Jr, Sexton, D. J., and Benkovic, S. J. 1997. Dissociation of bacteriophage T4 DNA polymerase and its processivity clamp after completion of Okazaki fragment synthesis. Biochemistry 36:14409–14417.

Cha, T.-A., and Alberts, B. M. 1986. Studies of the DNA helicase-RNA primase unit from bacteriophage T4. A trinucleotide sequence on the DNA template starts RNA primer synthesis. J. Biol. Chem. 261:7001–7010.

Cha, T.-A., and Alberts, B. M. 1989. The bacteriophage T4 DNA replication fork: only DNA helicase is required for leading strand DNA synthesis by the DNA polymerase holoenzyme. J. Biol. Chem. 264:12220–12225.

Cha, T.-A., and Alberts, B. M. 1990. Effects of the bacteriophage T4 gene 41 and gene 32 proteins on RNA primer synthesis: coupling of leading- and lagging-strand DNA synthesis at a replication fork. Biochemistry 29:1791–1798.

Chastain, P. D. 2nd, Makhov, A. M., Nossal, N. G., and Griffith, J. D. 2000. Analysis of the Okazaki fragment distributions along single long DNAs replicated by the bacteriophage T4 proteins. Mol. Cell. 6:803–814.

Chastain, P. D. 2nd, Makhov, A. M., Nossal, N. G., and Griffith, J. 2003. Architecture of the replication complex and DNA loops at the fork generated by the bacteriophage T4 proteins. J. Biol. Chem. 278:21276–21285.

Curtis, M. J., and Alberts, B. M. 1976. Studies on the structure of intracellular bacteriophage T4 DNA. J. Mol. Biol. 102:793–816.

Dong, F., Gogol, E. P., and von Hippel, P. H. 1995. The phage T4-coded DNA replication helicase (gp41) forms a hexamer upon activation by nucleoside triphosphate. J. Biol. Chem. 270:7462–7473.

Dong, F., and von Hippel, P.H. 1996. The ATP-activated hexameric helicase of bacteriophage T4 (gp41) forms a stable primosome with a single subunit of T4-coded primase (gp61). J. Biol. Chem. 271:19625–19631.

Dudas, K. C., and Kreuzer, K. N. 2005. Bacteriophage T4 helicase loader protein gp59 functions as gatekeeper in origin-dependent replication in vivo. J. Biol. Chem. 280: 21561–21569.

Egelman, E. H., Yu, X., Wild, R., Hingorani, M. M., and Patel, S. S. 1995. Bacteriophage T7 helicase/primase proteins form rings around single-stranded DNA that suggest a general structure for hexameric helicases. Proc. Natl. Acad. Sci. USA 92:3869–3873.

Epstein, R. H., Bolle, A., Steinberg, C. M., Kellenberger, E., Boy de la Tour, E., Chevalley, R., Edgar, R. S., Susman, M., Denhardt, G. H., and Lielausis, A. 1963. Physiological studies of conditional lethal mutants of bacteriophage T4D. Cold Spring Harbor Symp. Quant. Biol. 28:375–392.

Formosa, T., Burke, R. L., and Alberts, B. M. 1983. Affinity purification of bacteriophage T4 proteins essential for DNA replication and genetic recombination. Proc. Nat. Acad. Sci. USA 80:2442–2446.

Franklin, M. C., Wang, J., and Steitz, T. A. 2001. Structure of the replicating complex of a pol alpha family DNA polymerase. Cell 105:657–667.

Giedroc, D. P., Khan, R., and Barnhart, K. 1990. Overexpression, purification, and characterization of recombinant T4 gene 32 protein 22–301 (g32P-B). J. Biol. Chem. 265:11444–11455.

Gold, L., O'Farrell, P. Z., and Russel, M. 1976. Regulation of gene 32 expression during bacteriophage T4 infection of *Escherichia coli*. J. Biol. Chem. 251:7251–7262.

Goodrich, L. D., Lin, T. C., Spicer, E. K., Jones, C., and Konigsberg, W. H. 1997. Residues at the carboxy terminus of T4 DNA polymerase are important determinants for interaction with the polymerase accessory proteins. Biochemistry 36:10474–10481.

Hacker, K. J., and Alberts, B. M. 1994. The rapid dissociation of the T4 DNA polymerase holoenzyme when stopped by a DNA hairpin helix. A model for polymerase release following the termination of each Okazaki fragment. J. Biol. Chem. 269:24221–24228.

Hardman, C. H., Broadhurst, R. W., Raine, A. R., Grasser, K. D., Thomas, J. O., and Laue, E. D. 1995. Structure of the A-domain of HMG1 and its interaction with DNA as studied by heteronuclear three- and four-dimensional NMR spectroscopy. Biochemistry 34:16596–16607.

Hinton, D. M., and Nossal, N. G. 1987. Bacteriophage T4 DNA primase-helicase. Characterization of oligomer synthesis by T4 61 protein alone and in conjunction with T4 41 protein. J. Biol. Chem. 262:10873–10878.

Huberman, J. A., Kornberg, A., and Alberts, B. M. 1971. Stimulation of T4 bacteriophage DNA polymerase by the protein product of T4 gene 32. J. Mol. Biol. 62:39–52.

Ishmael, F. T., Alley, S. C., and Benkovic, S. J. 2001. Identification and mapping of protein-protein interactions between gp32 and gp59 by cross-linking. J. Biol. Chem. 276:25236–25242.

Ishmael, F. T., Alley, S. C., and Benkovic, S. J. 2002. Assembly of the bacteriophage T4 helicase: architecture and stoichiometry of the gp41–gp59 complex. J. Biol. Chem. 277:20555–20562.

Ishmael, F. T., Trakselis, M. A., and Benkovic, S. J. 2003. Protein–protein interactions in the bacteriophage T4 replisome. The leading strand holoenzyme is physically linked to the lagging strand holoenzyme and the primosome. J. Biol. Chem. 278:3145–3152.

Janzen, D. M., Torgov, M. Y., and Reddy, M. K. 1999. In vitro reconstitution of the bacteriophage T4 clamp loader complex (gp44/62). J. Biol. Chem. 274:35938–35943.

Jeruzalmi, D., Yurieva, O., Zhao, Y., Young, M., Stewart, J., Hingorani, M., O′Donnell M., and Kuriyan, J. 2001. Mechanism of processivity clamp opening by the delta subunit wrench of the clamp loader complex of *E. coli* DNA polymerase III. Cell 106:417–428.

Jing, D. H., Dong, F., Latham, G. J., and von Hippel, P. H. 1999. Interactions of bacteriophage T4-coded primase (gp61) with the T4 replication helicase (gp41) and DNA in primosome formation. J. Biol. Chem. 274:27287–27298.

Jing, D., Beechem, J. M., and Patton, W. F. 2004. The utility of a two-color fluorescence electrophoretic mobility shift assay procedure for the analysis of DNA replication complexes. Electrophoresis 25:2439–2446.

Jones, C. E., Mueser, T. C., and Nossal, N. G. 2000. Interaction of the bacteriophage T4 gene 59 helicase loading protein and gene 41 helicase with each other and with fork, flap and cruciform DNA. J. Biol. Chem. 275:27145–27154.

Jones, C. E., Green, E. M., Stephens, J. A., Mueser, T. C., and Nossal, N. G. 2004a. Mutations of bacteriophage T4 59 helicase loader defective in binding fork DNA and in interactions with T4 32 single-stranded DNA-binding protein. J. Biol. Chem. 279:25721–25728.

Jones, C. E., Mueser, T. C., and Nossal, N. G. 2004b. Bacteriophage T4 32 protein is required for helicase-dependent leading strand synthesis when the helicase is loaded by the T4 59 helicase-loading protein. J. Biol. Chem. 279:12067–12075.

Kaboord, B. F., and Benkovic, S. J. 1993. Rapid assembly of the bacteriophage T4 core replication complex on a linear primer/template construct. Proc. Natl. Acad. Sci. USA 90:10881–10885.

Kadyrov, F. A., and Drake, J. W. 2001. Conditional coupling of leading-strand and lagging-strand DNA synthesis at bacteriophage T4 replication forks. J. Biol. Chem. 276:29559–29566.

Kato, M., Frick, D. N., Lee, J., Tabor, S., Richardson, C. C., and Ellenberger, T. 2001. A complex of the bacteriophage T7 primase-helicase and DNA polymerase directs primer utilization. J. Biol. Chem. 276:21809–21820.

Kelly, R. C., Jensen, D. E., and von Hippel, P. H. 1976. DNA "melting" proteins. IV. Fluorescence measurements of binding parameters for bacteriophage T4 gene 32-protein to mono-, oligo-, and polynucleotides. J. Biol. Chem. 251:7240–7250.

Kowalczykowski, S. C., Lonberg, N., Newport, J. W., Paul, L. S., and von Hippel, P. H. 1980. On the thermodynamics and kinetics of the cooperative binding of bacteriophage T4-coded gene 32 (helix destabilizing) protein to nucleic acid lattices. Biophys. J. 32:403–418.

Kreuzer, K. N., and Morrical, S. W. 1994. In Molecular Biology of Bacteriophage T4, ed. J. Karan, pp. 28–42. Washington, D. C.: American Society for Microbiology.

Kreuzer, K. N. 2000. Recombination-dependent DNA replication in phage T4. Trends. Biochem. Sci. 25:165–173.

Kusakabe, T., and Richardson, C. C. 1996. The role of the zinc motif in sequence recognition by DNA primases. J. Biol. Chem. 271:19563–19570.

Latham, G. J., Bacheller, D. J., Pietroni, P., and von Hippel, P. H. 1997a. Structural analyses of gp45 sliding clamp interactions during assembly of the bacteriophage T4 DNA polymerase holoenzyme. II. The Gp44/62 clamp loader interacts with a single defined face of the sliding clamp ring. J. Biol. Chem. 272:31677–31684.

Latham, G. J., Bacheller, D. J., Pietroni, P., and von Hippel, P. H. 1997b. Structural analyses of gp45 sliding clamp interactions during assembly of the bacteriophage T4 DNA polymerase holoenzyme. III. The Gp43 DNA polymerase binds to the same face of the sliding clamp as the clamp loader. J. Biol. Chem. 272:31685–31692.

Lefebvre, S. D., and Morrical, S. W. 1997. Interactions of the bacteriophage T4 gene 59 protein with single-stranded polynucleotides: binding parameters and ion effects. J. Mol. Biol. 272:312–326.

Lefebvre, S. D., Wong, M. L., and Morrical, S. W. 1999. Simultaneous interactions of bacteriophage T4 DNA replication proteins gp59 and gp32 with single-stranded (ss) DNA. Comodulation of ssDNA binding activities in a DNA helicase assembly intermediate. J. Biol. Chem. 274:22830–22838.

Lin, T. C., Karam, G., and Konigsberg, W. H. 1994. Isolation, characterization, and kinetic properties of truncated forms of T4 DNA polymerase that exhibit 3′-5′ exonuclease activity. J. Biol. Chem. 269:19286–19294.

Liu, C.-C., and Alberts, B. M. 1980. Pentaribonucleotides of mixed sequence are synthesized and efficiently prime de novo DNA chain starts in the T4 bacteriophage DNA replication system. Proc. Natl. Acad. Sci. USA 77:5698–5702.

Liu, C.-C., and Alberts, B. M. 1981a. Characterization of the DNA-dependent GTPase activity of T4 gene 41 protein, and essential component of the T4 bacteriophage DNA replication apparatus. J. Biol. Chem. 256:2813–2820.

Liu, C.-C., and Alberts, B. M. 1981b. Characterization of RNA primer synthesis in the T4 bacteriophage in vitro DNA replication system. J. Biol. Chem. 256:2821–2829.

Ma, Y., Wang, T., Villemain, J. L., Giedroc, D. P., and Morrical, S. W. 2004. Dual functions of single-stranded DNA-binding protein in helicase loading at the bacteriophage T4 DNA replication fork. J. Biol. Chem. 279:19035–19045.

Mace, D. C., and Alberts, B. M. 1984. T4 DNA polymerase rates and processivity on single-stranded DNA templates. J. Mol. Biol. 177:295–311.

Millar, D., Trakselis, M. A., and Benkovic, S. J. 2004. On the solution structure of the T4 sliding clamp (gp45). Biochemistry 43:12723–12727.

Miller, E. S., Kutter, E., Mosig, G., Arisaka, F., Kunisawa, T., and Ruger, W. 2003. Bacteriophage T4 genome. Microbiol. Mol. Biol. Rev. 67:86–156.

Moarefi, I., Jeruzalmi, D., Turner, J., O′Donnell, M., and Kuriyan, J. 2000. Crystal structure of the DNA polymerase processivity factor of T4 bacteriophage. J. Mol. Biol. 296:1215–1223.

Morrical, S. W., Hempstead, K., and Morrical, M. D. 1994. The gene 59 protein of bacteriophage T4 modulates the intrinsic and single–stranded DNA-stimulated ATPase activities of gene 41 protein, the T4 replicative DNA helicase. J. Biol. Chem. 269:33069–33081.

Morrical, S. W., Beernink, H. T., Dash, A., and Hempstead, K. 1996. The gene 59 protein of bacteriophage T4. Characterization of protein-protein interactions with gene 32 protein, the T4 single-stranded DNA binding protein. J. Biol. Chem. 271:20198–20207.

Morris, P. D., and Raney, K. D. 1999. DNA helicases displace streptaviding from biotin-labeled oligonucleotides. Biochemistry 38:5164–5171.

Mueser, T. C., Jones, C. E., Nossal, N. G., and Hyde, C. C. 2000. Bacteriophage T4 gene 59 helicase assembly protein binds replication fork DNA. The 1.45 Å resolution crystal structure reveals a novel alpha-helical two-domain fold. J. Mol. Biol. 296:597–612.

Nelson, S. W., Yang, J., and Benkovic, S. J. 2006. Site-directed mutations of T4 helicase loading protein (gp59) reveal multiple modes of DNA polymerase inhibition and the mechanism of unlocking by gp41 helicase. J. Biol. Chem. 281:8697–8706.

Norcum, M. T., Warrington, J. A., Spiering, M. M., Ishmael, F. T., Trakselis, M. A., and Benkovic, S. J. 2005. Architecture of the bacteriophage T4 primosome: electron microscopy studies of helicase (gp41) and primase (gp61). Proc. Natl. Acad. Sci. USA 102:3623–3626.

Nossal, N. G. 1980. RNA priming of DNA replication by bacteriophage T4 proteins. J. Biol. Chem. 255:2176–2182.

Nossal, N. G., Dudas, K. C., and Kreuzer, K. N. 2001. Bacteriophage T4 proteins replicate plasmids with a preformed R loop at the T4 ori(uvsY) replication origin in vitro. Mol. Cell 7:31–41.

Pietroni, P., Young, M. C., Latham, G. J., and von Hippel, P. H. 2001. Dissection of the ATP-driven reaction cycle of the bacteriophage T4 DNA replication processivity clamp loading system. J. Mol. Biol. 309:869–891.

Raney, K. D., Carver, T. E., and Benkovic, S. J. 1996. Stoichiometry and DNA unwinding by the bacteriophage T4 41:59 helicase. J. Biol. Chem. 271:14074–14081.

Richardson, C. C., and Nossal, N. G. 1989. Characterization of the bacteriophage T4 gene 41 DNA helicase. J. Biol. Chem. 264:4725–4731.

Stasiak, A., Tsaneva, I. R., West, S. C., Benson, C. J., Yu, S., and Egelman, E. H. 1994. The *Escherichia coli* RuvB branch migration protein forms double hexameric rings around DNA. Proc. Natl. Acad. Sci. USA 91:7618–7622.

Schrock, R. D., and Alberts, B. M. 1996. Processivity of the gene 41 DNA helicase at the bacteriophage T4 DNA replication fork. J. Biol. Chem. 271:16678–16682.

Shamoo, Y., Friedman, A. M., Parsons, M. R., Konigsberg, W. H., and Steitz, T.A. 1995. Crystal structure of a replication fork single-stranded DNA binding protein (T4 gp32) complexed to DNA. Nature 376:362–366.

Shamoo, Y., and Steitz, T. A. 1999. Building a replisome from interacting pieces: sliding clamp complexed to a peptide from DNA polymerase and a polymerase editing complex. Cell 99:155–166.

Smiley, R. D., Zhuang, Z., Benkovic, S. J., and Hammes, G. G. 2006. Single-molecule investigation of the T4 bacteriophage DNA polymerase holoenzyme: multiple pathways of holoenzyme formation. Biochemistry 45:7990–7997.

Spacciapoli, P., and Nossal, N. G. 1994. Interaction of DNA polymerase and DNA helicase within the bacteriophage T4 DNA replication complex. Leading strand synthesis by the T4 DNA polymerase mutant A737V (tsL141) requires the T4 gene 59 helicase assembly protein. J. Biol. Chem. 269:447–455.

Trakselis, M. A., Alley, S. C., Abel-Santos, E., and Benkovic, S. J. 2001. Creating a dynamic picture of the sliding clamp during T4 DNA polymerase holoenzyme assembly by using fluorescence resonance energy transfer. Proc. Natl. Acad. Sci. USA 98:8368–8375.

Trakselis, M. A., Berdis, A. J., and Benkovic, S. J. 2003a. Examination of the role of the clamploader and ATP hydrolysis in the formation of the bacteriophage T4 polymerase holoenzyme. J. Mol. Biol. 326:435–451.

Trakselis, M. A., Roccasecca, R. M., Yang, J., Valentine, A. M., and Benkovic, S. J. 2003b. Dissociative properties of the proteins within the bacteriophage T4 replisome. J. Biol. Chem. 278:49839–49849.

Valentine, A. M., Ishmael, F. T., Shier, V. K., and Benkovic, S. J. 2001. A zinc ribbon protein in DNA replication: primer synthesis and macromolecular interactions by the bacteriophage T4 primase. Biochemistry 40:15074–15085.

Venkatesan, M., Silver, L. L., and Nossal, N. G. 1982. Bacteriophage T4 gene 41 protein, required for the synthesis of RNA primers, is also a DNA helicase. J. Biol. Chem. 257:12426–12434.

Wang, J., Sattar, A. K., Wang, C. C., Karam, J. D., Konigsberg, W. H., and Steitz, T. A. 1997. Crystal structure of a pol alpha family replication DNA polymerase from bacteriophage RB69. Cell 89:1087–1099.

Wu, J. R., and Yeh, Y. C. 1975. New Late Gene, *dar*, Involved in DNA Replication of Bacteriophage T4 I. Isolation, Characterization, and Genetic Location. J. Virol. 15:1096–1106.

Wu, C. A., Zechner, E. L., Reems, J. A., McHenry, C. S., and Marians, K. J. 1992. Coordinated leading- and lagging-strand synthesis at the *Escherichia coli* DNA replication fork. V. Primase action regulates the cycle of Okazaki fragment synthesis. J. Biol. Chem. 267: 4074–4083.

Xi, J., Zhuang, Z., Zhang, Z., Selzer, T., Spiering, M. M., Hammes, G. G., and Benkovic, S. J. 2005a. Interaction between the T4 helicase-loading protein (gp59) and the DNA polymerase (gp43): a locking mechanism to delay replication during replisome assembly. Biochemistry 44:2305–2318.

Xi, J., Zhang, Z., Zhuang, Z., Yang, J., Spiering, M. M., Hammes, G. G., and Benkovic, S. J. 2005b. Interaction between the T4 helicase loading protein (gp59) and the DNA polymerase (gp43): unlocking of the gp59-gp43-DNA complex to initiate assembly of a fully functional replisome. Biochemistry 44:7747–7756.

Xu, H., Wang, Y., Bleuit, J. S., and Morrical, S. W. 2001. Helicase assembly protein Gp59 of bacteriophage T4: fluorescence anisotropy and sedimentation studies of complexes formed with derivatives of Gp32, the phage ssDNA binding protein. Biochemistry 40:7651–7661.

Yang, J., Trakselis, M. A., Roccasecca, R. M., and Benkovic, S. J. 2003. The application of a minicircle substrate in the study of the coordinated T4 DNA replication. J. Biol. Chem. 278:49828–49838.

Yang, J., Zhuang, Z., Roccasecca, R. M., Trakselis, M. A., and Benkovic, S. J. 2004. The dynamic processivity of the T4 DNA polymerase during replication. Proc. Natl. Acad. Sci. USA 101:8289–8294.

Yang, J., Xi, J., Zhuang, Z., and Benkovic, S. J. 2005. The oligomeric T4 primase is the functional form during replication. J. Biol. Chem. 280:25416–25423.

Yang, J., Nelson, S. W., and Benkovic, S. J. 2006. The control mechanism for lagging strand polymerase recycling during bacteriophage T4 DNA replication. Mol. Cell 21:153–164.

Yao, N., Turner, J., Kelman, Z., Stukenberg, P. T., Dean, F., Shechter, D., Pan, Z. Q., Hurwitz, J., and O′Donnell, M. 1996. Clamp loading, unloading and intrinsic stability of the PCNA, beta and gp45 sliding clamps of human, *E. coli* and T4 replicases. Genes Cells 1:101–113.

Yegian, C. D., Mueller, M., Selzer, G., Russo, V., and Stahl, F. W. 1971. Properties of the DNA-delay mutants of bacteriophage T4. Virology 46:900–919.

Yonesaki, T. 1994. The purification and characterization of gene 59 protein from bacteriophage T4. J. Biol. Chem. 269:1284–1289.

Young, M. C., Schultz, D. E., Ring, D., and von Hippel, P. H. 1994. Kinetic parameters of the translocation of bacteriophage gene 41 protein helicase on single-stranded DNA. J. Mol. Biol. 235:1447–1458.

Yuzhakov, A., Kelman, Z., and O′Donnell, M. 1999. Trading places on DNA – a three-point switch underlies primer handoff from primase to the replicative DNA polymerase. Cell. 96:153–163.

Zhang, Z., Spiering, M. M., Trakselis, M. A., Ishmael, F. T., Xi, J., Benkovic, S. J., and Hammes, G. G. 2005. Assembly of the bacteriophage T4 primosome: single-molecule and ensemble studies. Proc. Natl. Acad. Sci. USA 102:3254–3259.

Zhuang, Z., Berdis, A. J., and Benkovic, S. J. 2006a. An alternative clamp loading pathway via the T4 clamp loader gp44/62-DNA complex. Biochemistry 45:7976–7989.

Zhuang, Z., Yoder, B. L., Burgers, P. M., and Benkovic, S. J. 2006b. The structure of a ring-opened proliferating cell nuclear antigen-replication factor C complex revealed by fluorescence energy transfer. Proc. Natl. Acad. Sci. USA 103:2546–2551.